nature cell biology

# Polycomb response elements mediate the formation of chromosome higher-order structures in the bithorax complex

Chiara Lanzuolo[1], Virginie Roure[2], Job Dekker[3], Frédéric Bantignies[2] and Valerio Orlando[1,4]

**In *Drosophila*, the function of the Polycomb group genes (PcGs) and their target sequences (Polycomb response elements (PREs)) is to convey mitotic heritability of transcription programmes — in particular, gene silencing. As part of the mechanisms involved, PREs are thought to mediate this transcriptional memory function by building up higher-order structures in the nucleus. To address this question, we analysed *in vivo* the three-dimensional structure of the homeotic locus bithorax complex (BX-C) by combining chromosome conformation capture (3C) with fluorescent *in situ* hybridization (FISH) and FISH immunostaining (FISH-I) analysis. We found that, in the repressed state, all major elements that have been shown to bind PcG proteins, including PREs and core promoters, interact at a distance, giving rise to a topologically complex structure. We show that this structure is important for epigenetic silencing of the BX-C, as we find that major changes in higher-order structures must occur to stably maintain alternative transcription states, whereas histone modification and reduced levels of PcG proteins determine an epigenetic switch that is only partially heritable.**

The genes of the Polycomb group (PcG) code for chromatin multiprotein complexes that prevent changes in transcription programmes, thus preserving cell identity[1]. In *Drosophila*, PcG function is mediated by specialized epigenetic DNA modules, called Polycomb response elements (PREs), that control promoters at a distance via chromatin structure and interference with RNA Polymerase II[2,3]. Notably, these long-distance effects seem to occur both *in cis* and *in trans*[4–6]. Thus, it has been suggested that a crucial mechanistic aspect of PcG proteins and PREs would be to create higher-order structures[7]. This level of chromosome organization could be essential for epigenetic inheritance[8]. To test this hypothesis, we used fluorescent *in situ* hybridization (FISH), FISH with immunostaining (FISH-I) and chromosome conformation capture (3C) technologies to investigate physical and spatial interactions between regulatory regions of the homeotic bithorax complex (BX-C).

The 340 kilobases (kb) encompassing the BX-C contains both protein-coding and non-coding transcription units, each controlled by several regulatory elements that specify the parasegment activity of three genes — *Ultrabithorax* (*Ubx*), *abdominalA* (*abdA*) and *AbdominalB* (*AbdB*). Regulated non-coding transcription units overlap PREs and promoters, and directly participate in PcG-mediated epigenetic inheritance[9–11]. Thus, a complex network of interactions between *cis*-regulatory elements is likely to occur. Indeed, higher-order interactions between BX-C regulatory regions in both the active and the repressed state have been described. These involve specific insulator–promoter and enhancer–promoter interactions[5,6,12]. *Trans*-sensing effects among homologous PREs were reported[4,13]. However, it is not clear whether or not PRE–PRE interactions also occur in non-homologous DNA elements and their role in epigenetic regulation.

We first addressed this issue at low resolution by two-colour FISH analysis. We looked at different parts of wild-type 5–8 h staged embryos, in which the expression of BX-C genes differs depending on the parasegment observed. At this stage, homeotic gene patterning is completed and the PcG-mediated memory system has already initiated. We used two FISH probes spanning the *bxd* and the *Fab-7* PREs that control the *Ubx* and *AbdB* genes, respectively, separated *in vivo* by approximately 130 kb. The measurements of the distance between the two signals indicate that *bxd* and *Fab-7* are colocalized well in tissues where *AbdB* and *Ubx* are repressed (head of the embryo). Conversely, in the abdominal parasegments (13–14) of the embryo, where *AbdB* is active and *Ubx* is silenced, the two elements are mostly separated (Fig. 1a,b). There is increasing evidence that repositioning of genomic regions with respect to nuclear compartments is important for the regulation of gene expression[8,14–16]. PcG proteins are found in discrete bodies in the nucleus[17,18]. We investigated the nuclear position of differently transcribed BX-C loci relative to Polycomb bodies. We used two-colour

[1]Dulbecco Telethon Institute at IGB CNR, Epigenetics and Genome Reprogramming, Via Pietro Castellino 111, 80131 Naples, Italy; [2]Institute of Human Genetics, Chromatin and Cell Biology lab, UPR 1142 — CNRS, 141 rue de la Cardonille, 34396 Montpellier — Cedex 5, France; [3]Program in Gene Function and Expression, Department of Biochemistry and Molecular Pharmacology, University of Massachusetts Medical School, Worcester, Massachusetts 01605, USA.
[4]Correspondence should be addressed to V.O. (orlando@igb.cnr.it)

Received 12 March 2007; accepted 26 July 2007; published online 9 September 2007; DOI: 10.1038/ncb1637

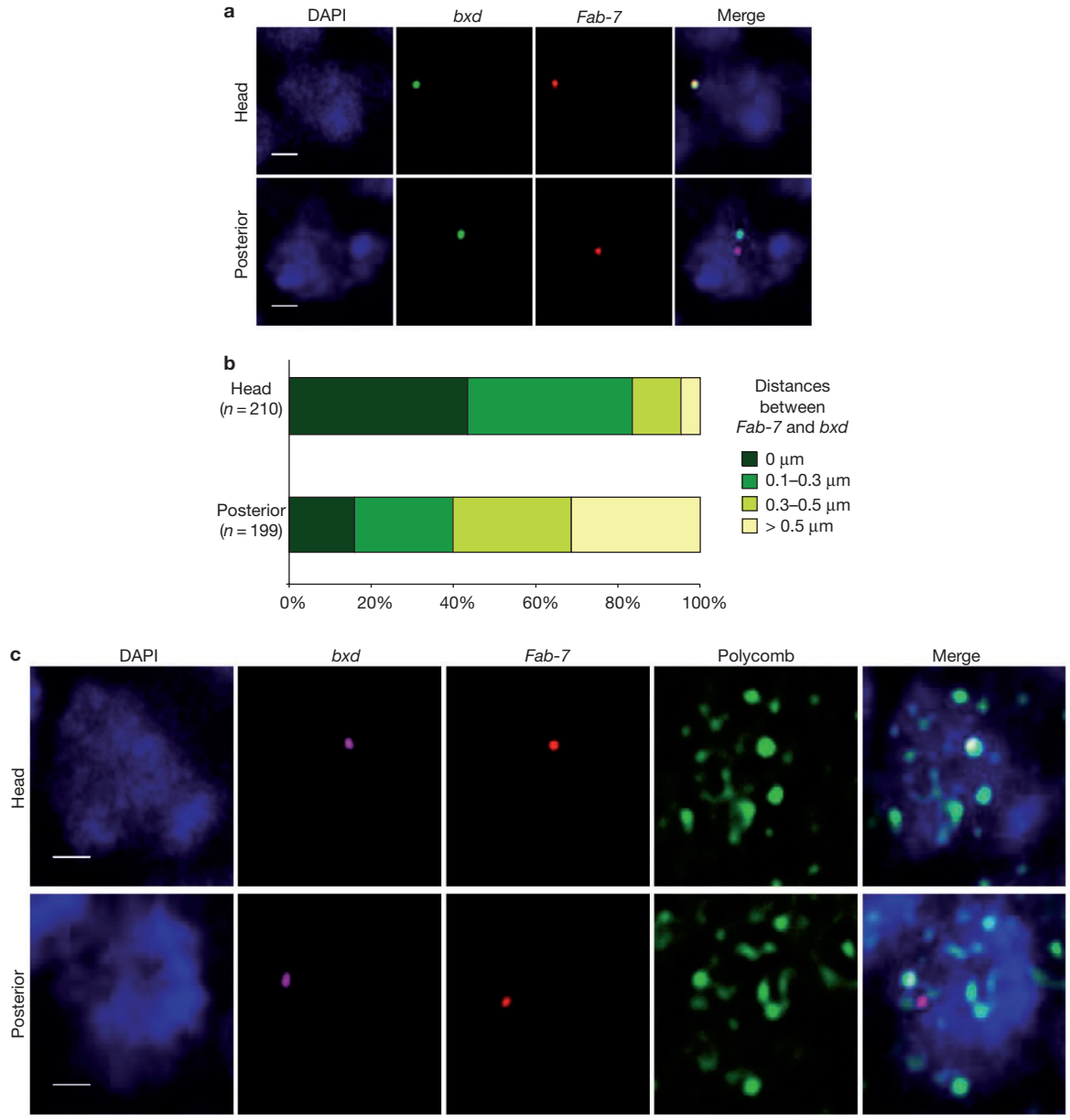


**Figure 1** Repressed PREs colocalize in PC bodies. (**a**) Representative examples of individual nuclei. DAPI staining, the *bxd* element, the *Fab-7* element and the merge of the three channels are shown. (**b**) Two-colour fluorescent *in situ* hybridization (FISH) in wild-type 5–8 h staged embryos. Percentage of distances between *Ubx* and *Abd-B* loci. The 0 µm category represents overlapping signals and the 0.1–0.3 µm category represents paired signals. A total of 60–70 nuclei per embryo from three different embryos were analysed in each case. *n* indicates the total number of nuclei analysed. Two-sample Kolmogorov–Smirnov was applied for statistical analysis (D=0.4193; $P = 2.44*10^{-13}$). (**d**) Distinct nuclear organization of *bxd* and *Fab-7* elements in the head and the posterior part of the embryo. Characteristic individual nuclei with two-colour FISH with immunostaining. DAPI staining, *bxd, Fab-7*, the PC bodies, and the merge of the four channels are shown. Scale bars, 1 µm.

FISH and FISH-I in whole-mount wild-type embryos, using *Fab-7* and *bxd* as FISH probes. We found that the two repressed elements colocalize in a large Polycomb body in more than 80% of the anterior nuclei analysed (Fig. 1c). Conversely, in the posterior part of the embryos, *bxd* remains colocalized in a PcG body in 80% of nuclei, whereas *Fab-7* is clearly outside this domain in 90% of cases.

The colocalization between PREs in the inactive state might correspond to compaction of the BX-C — perhaps as a consequence of specific interactions between regulatory elements, including PREs. To investigate the interactions occurring between different regulatory elements of the BX-C and to determine the overall topological conformation of the repressed BX-C *in vivo*, we applied the high-resolution 3C technique in embryos. To this, formaldehyde-fixed chromatin was prepared from 5–8 h staged embryos. We started an unbiased 3C walk analysis along the 340 kb encompassing the BX-C by using a *Hind*III fragment containing the *abdA* promoter as 'bait' (fragment 28; Fig. 2), which is located in the centre of the cluster. We measured the cross-linking frequencies between this element and the 59 other *Hind*III fragments of the BX-C complex (Fig. 2a; see also Methods). As an internal control, in the same analysis, we also measured the cross-linking frequencies with *Hind*III fragments covering 80 kb upstream of the BX-C complex, a region that does not contain homeotic genes.

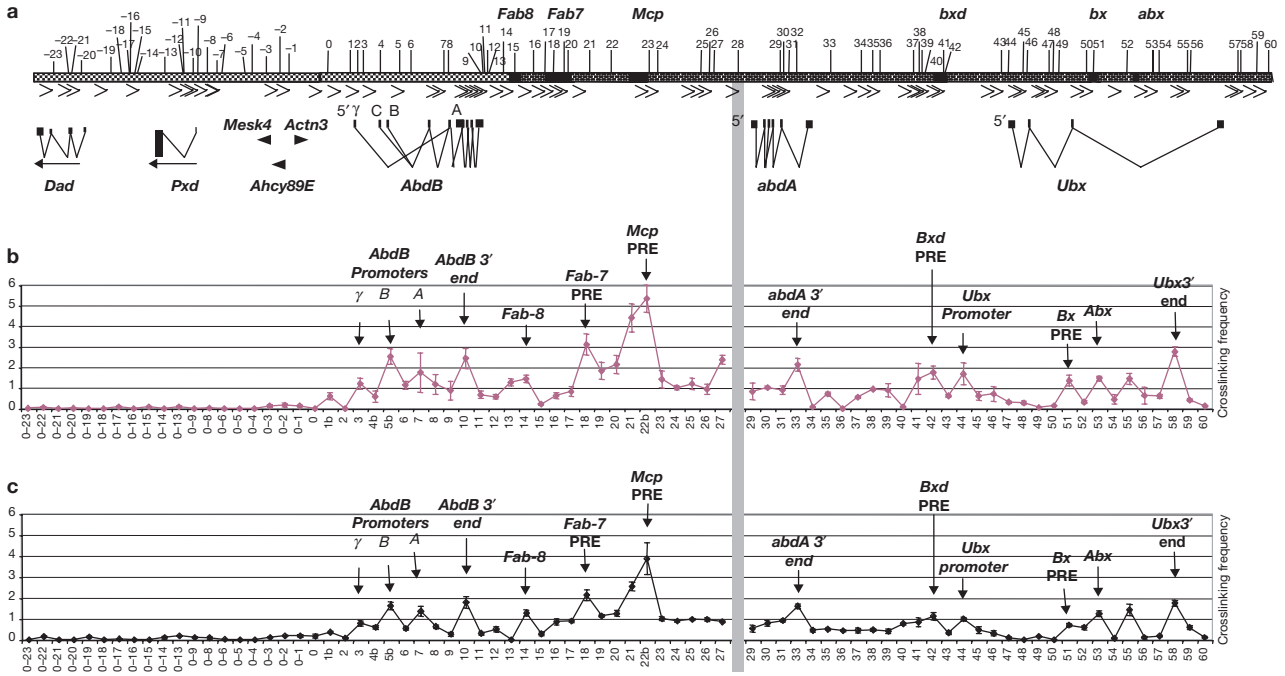


**Figure 2** BX-C conformation in staged embryos. (**a**) The scheme shows the bithorax complex (BX-C), including transcription units and genetically characterized regulatory regions. Black arrows represent the positions of the primers used. Numbers indicate *Hind*III sites. The grey bar marks the position of the fixed primer. (**b**) Crosslinking frequencies between the fixed *Hind*III fragment 28 (*abdA* promoter) and the rest of the locus in embryos. All data points were generated from an average of four different experiments. Standard error of the mean is indicated. One-way ANOVA was applied for statistical analysis; α= 0.05. ($P = 1.87*10^{-23}$); F(58,227)=6,99. (**c**) Crosslinking frequencies between the fixed *Hind*III fragment 28 (*abdA* promoter) and the rest of the locus in S2 cells. All data points were generated from an average of six different experiments (with a minimum of three). ($P = 0.96*10^{-55}$); F(58,457)=11,49.

Importantly, the cross-linking frequencies of the *abdA* promoter with the control region were close to the zero value (Fig. 2b). This suggests that the BX-C locus forms a topologically distinct structure that does not share contacts with the flanking, non-homeotic genes.

We found a tight association between the *abdA* promoter and the *Mcp* PRE (fragment 22b), confirming the idea that PREs physically interact with promoters[5,6]. Strikingly, the *abdA* promoter also interacts with all major elements in the BX-C that bind PcG proteins, including PREs/boundary elements (*Fab-8*, fragment 14; *Fab-7*, fragment 18; *bxd*, fragment 42; *bx*, fragment 51; *abx*, fragment 53), and the other homeotic gene promoters (*AbdB* γ promoter, fragment 1b/3; *AbdB* B promoter, fragment 5b; *AbdB* A promoter, fragment 7; *Ubx* promoter, fragment 44). Interestingly, the *abdA* promoter also interacts with the 3' end of all three homeotic BX-C genes (*AbdB* 3' end, fragment 10; *abdA* 3' end, fragment 33; *Ubx* 3' end, fragment 58), and with an unknown element located within the largest intronic region of *Ubx* (fragment 55). This analysis suggests that the BX-C is potentially folded in topologically ordered and discrete domains that are mediated by all major PcG DNA-binding elements. The quantitative differences in the cross-linking values between different regions seem to reflect different levels of higher-order structure, where epigenetic elements that are functionally related are also spatially closer.

In *Drosophila* embryos, these 3C data would virtually represent all interactions occurring between BX-C regulatory elements in embryonic nuclei due to the intrinsic differences in the expression of BX-C genes along the anterior–posterior axis of the embryo. To measure the interactions occurring only in the fully repressed state, we examined cultured embryonic cells. In the Schneider 2 line (S2) used in this study, *Ubx, abdA* and *AbdB* are repressed, thus providing a homogeneous cell population with a complete silenced BX-C complex[19]. We found a highly comparable profile to the one found in embryos (Fig. 2c), in which the *abdA* promoter interacts with all PREs, promoters and the 3' end of BX-C genes. This indicates that the profile obtained in embryos reflects the interactions occurring between repressed elements.

To validate this panel of long-range interactions, we used other genomic regions as 'baits' (see Supplementary Information, Figs S1, S2). We found, with different fixed primers, highly similar patterns along the BX-C. The profiles of interactions are not completely overlapping. For instance, the *abdA* promoter interacts with the other homeotic promoters, whereas the *AbdB* γ promoter (maybe for sterical reasons) does not clearly interact with the *Ubx* promoter. We conclude that the repressed BX-C complex adopts a specific multi-loop structure, which is organized in three domains corresponding to the three transcriptional units. In the repressed state, the homeotic promoter strongly interacts with its epigenetic regulatory elements (PREs) in each domain. In addition, PREs and the 3' end of homeotic genes mediate long-range chromosomal interactions between different domains. These data are the first evidence that non-homologous PREs physically interact with each other to build up higher-order structures corresponding to repressed domains.

To analyse the correlation between transcription and BX-C higher-order structures, we forced the reactivation of homeotic genes in cultured cells. The reduction of PcG protein synthesis by double-stranded RNA (dsRNA) in S2 cells induces loss of PC binding at PREs and derepression

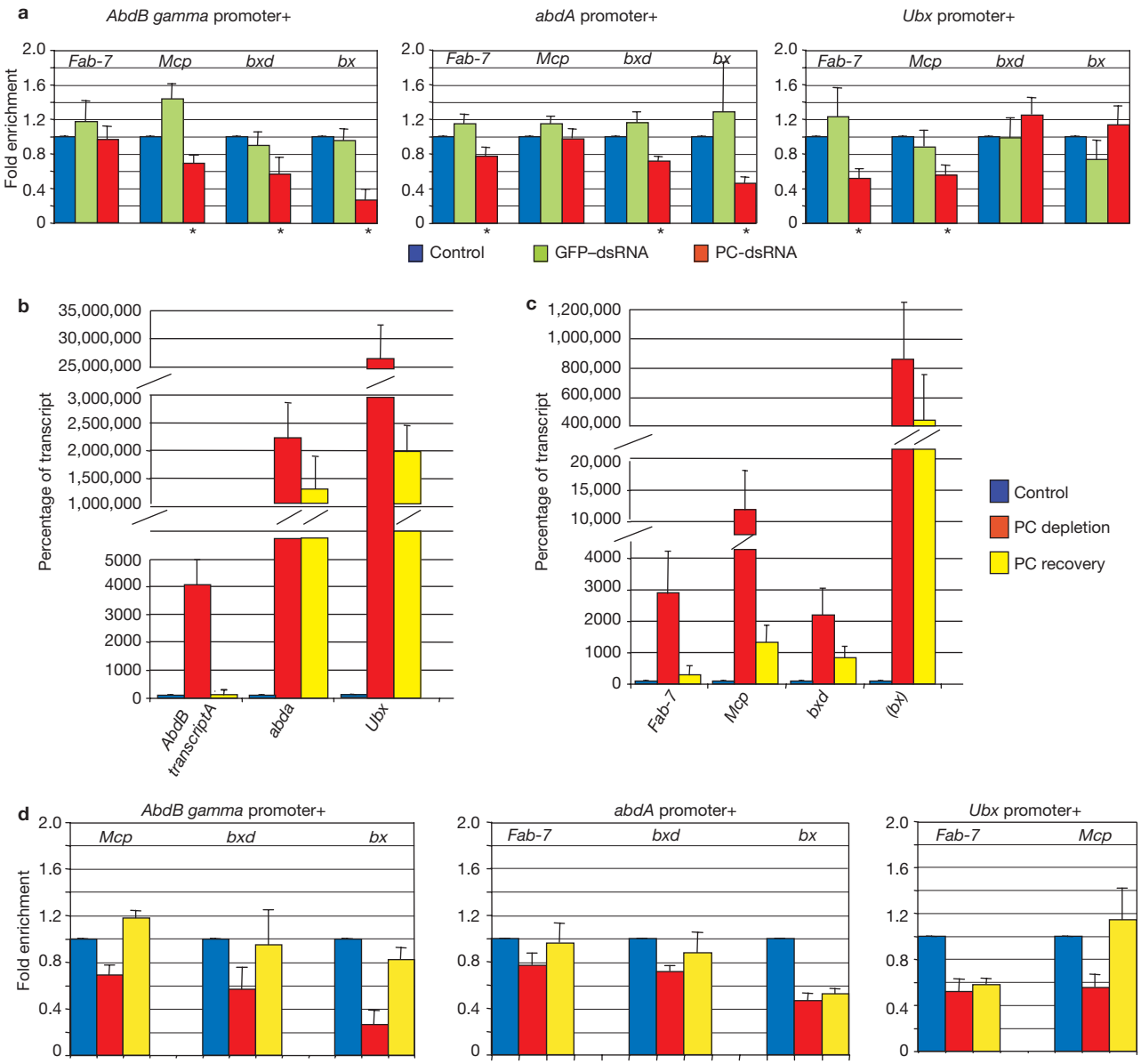


**Figure 3** PC depletion affects long-range interactions. (**a**) Crosslinking frequencies observed in mock RNA interference (RNAi) S2 cells (Control) are shown in blue. Data obtained in GFP–dsRNA-treated cells in green and PC-dsRNA-treated cells in red. Crosslinking frequencies, normalized on the control, between the fixed fragments spanning the three homeotic promoters (*AbdB* γ; *abdA*; *Ubx*) and bithorax complex Polycomb response elements (PREs). Standard error of the mean is indicated. Two-tailed *t*-test was applied for statistical analysis. Asterisks indicate the differences that are statistically relevant; α=0.05. *P* and *n values*: *AbdB* γ promoter/*Mcp*: $P = 0.9*10^{-3}$, $n = 8$; *AbdB* γ promoter/*bxd*: $P = 0.4*10^{-2}$, $n = 8$; *AbdB* γ promoter/*bx*: $P = 0.8*10^{-2}$, $n = 9$; *abdA* promoter/*Fab-7*: $P = 0.2*10^{-2}$, $n = 8$; *abdA* promoter/*bxd*: $P = 0.3*10^{-3}$, $n = 13$; *abdA* promoter/*bx*: $P = 0.3*10^{-4}$, $n = 16$; *Ubx* promoter/*Fab-7*: $P = 0.5*10^{-3}$, $n = 12$; *Ubx* promoter/*Mcp*: $P = 0.8*10^{-3}$, $n = 12$. (**b**) Quantification of transcripts by real-time PCR. Transcriptional levels are shown as a percentage of *Gadph* expression. All data points were generated from an average of four different experiments. Standard error of the mean is indicated. Expression level of homeotic genes in mock RNAi S2 cells (Control) (blue), in PC-dsRNA-treated cells relative to Control (red) and in recovered cells relative to Control (yellow). (**c**) Expression levels of PREs as in **a**. (**d**) Crosslinking frequencies, normalized on the control, between the fixed fragments spanning the three homeotic promoters (*AbdB* γ; *abdA*; *Ubx*) and distal PREs.

of homeotic genes[19,20]. To assess whether this 'artificial' gene activation can alter the putative superstructure of the BX-C, we applied the 3C assay on cells that had been 'knocked down' for Polycomb (PC), one of the major components of the PRC1 complex. As control, we used mock RNA interference (no dsRNA) (Control) and green fluorescent protein (GFP) dsRNA. After eight rounds of treatment with PC-dsRNA, the *Pc* transcript is reduced by 80% compared with the control, and we observed different levels of transcriptional activation of the homeotic genes (see Supplementary Information, Fig. S3a,b). As expected, concomitantly with the derepression of homeotic genes, we also found transcriptional activation occurring at PREs[11]. Interestingly, this PRE transcription is significantly lower than for naturally active PREs (see Supplementary Information, Fig. S3c,e). Following this, 3C analysis of PC and control samples was performed with the *abdA* promoter as bait (fragment 28;

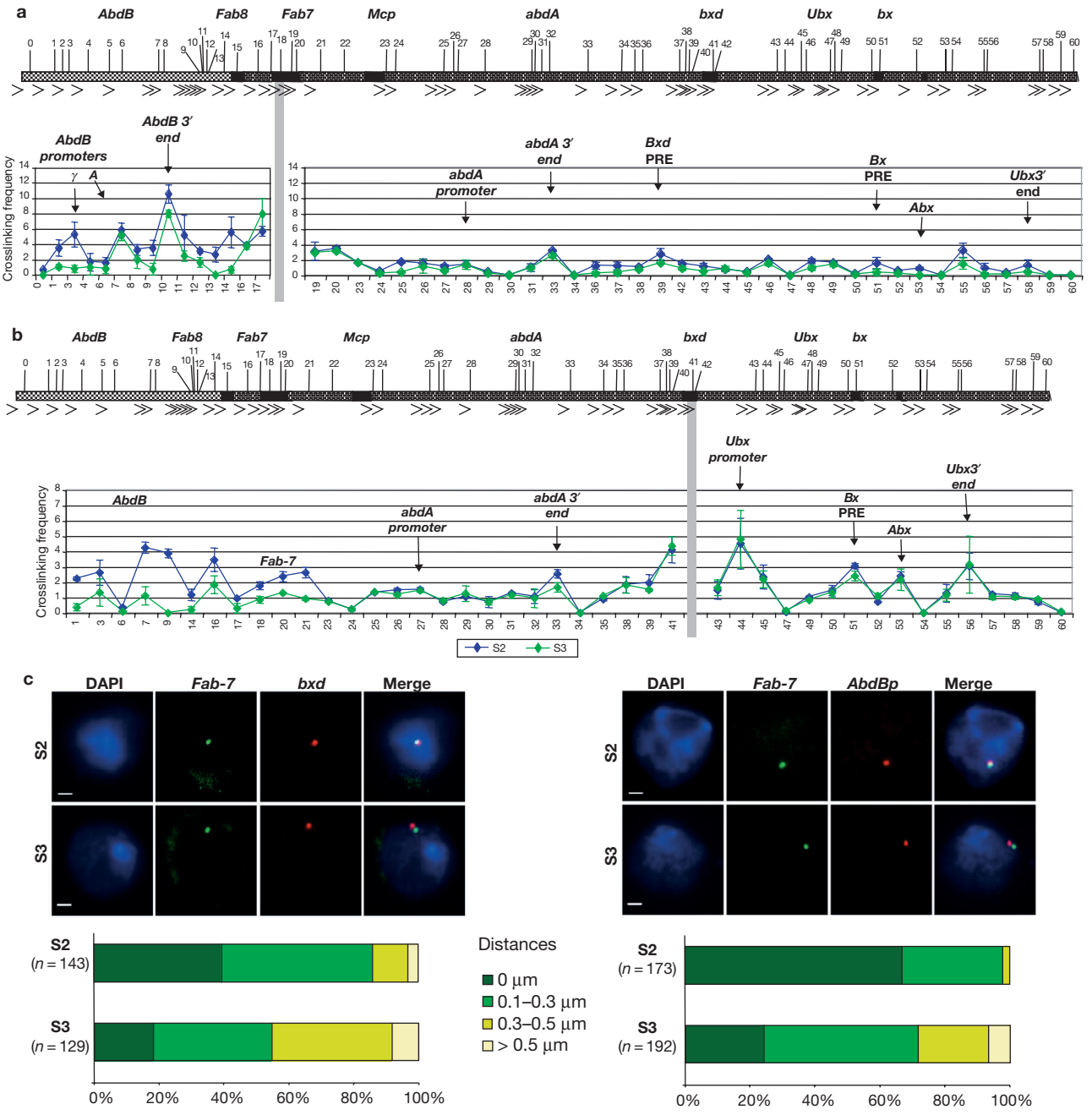


**Figure 4** Different BX-C conformations in constitutively active cells. The bithorax complex (BX-C) locus is shown on the top of each graph (see Fig. 1). Crosslinking frequencies observed in S2 cells are shown in blue. Data obtained in S3 cells are shown in green. All data points were generated from an average of four different experiments. Standard error of the mean is indicated. Two-way ANOVA was applied for statistical analysis; α=0.05. (**a**) Crosslinking frequencies between the fixed *Hind*III fragment 18 (*Fab-7* Polycomb response element (PRE)) and the rest of the locus ($P = 0.5*10^{-5}$). (**b**) Crosslinking frequencies between the fixed *Hind*III fragment 42 (*bxd* PRE) and the rest of the locus ($P = 0.002$). (**c**). Two-colour fluorescent *in situ* hybridization in S2 and S3 cells. Representative examples of individual nuclei. DAPI staining, the *bxd* element or the *AbdB* promoter, the *Fab-7* element, and the merge of the three channels are shown. Percentage of distances between *Fab-7* and *Ubx* or *Abd-B* loci. N indicates the total number of nuclei analysed. Two-sample Kolmogorov–Smirnov was applied for statistical analysis (*bxd-Fab-7*: D=0.4085, $P = 2.951*10^{-10}$; *AbdBp-Fab-7*: D=0.4419, $P = 7.772*10^{-16}$). Scale bars, 1 µm.

centre of the BX-C). No changes were observed in control samples (see Supplementary Information, Fig. S4b). The transcriptional reactivation of the BX-C, after PC depletion, was accompanied by specific changes in long-range interactions between the three homeotic transcriptional units (Fig. 3a, and see Supplementary Information, Fig. S4c). 3C analysis revealed, in fact, that after PC-dsRNA treatment the associations of the three active promoters (*AbdB* γ, *abdA* and *Ubx*) with the distal PREs are impaired (Fig. 3a). Conversely, the frequency of interaction between each promoter and proximal PRE elements (*AbdB*/*Fab-7*; *abdA*/*Mcp*; *Ubx*/*bx* or *bxd*) is not affected.

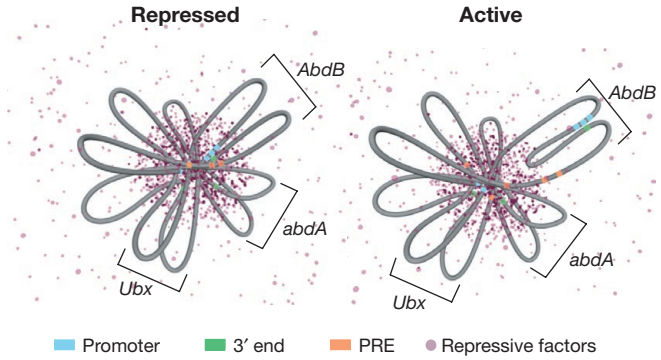


**Figure 5** The BX-C adopts different spatial conformations relative to its transcription state. In the repressed state, the bithorax complex (BX-C) locus adopts a condensed structure in which all the Polycomb group (PcG)-bound elements are interacting together. In this conformation, all Polycomb response elements (PREs; orange in the figure), promoters (light blue) and 3′ ends of the genes (green) organize the BX-C in topologically discrete domains. In cells with a constitutively active *AbdB* gene, the PRE–promoter interaction, observed in the context of repression, is lost, whereas the other epigenetic elements that are still silenced retain their clustered conformation.

To test the correlation between these structural changes and the ability to maintain, epigenetically, the switched state after stopping RNAi treatment, we kept the cells in culture for an additional month (almost 20 cell divisions) to restore normal PC levels. In all the independent clones that we followed after PC recovery, we found a global tendency to recover transcriptional repression of homeotic genes, with, in particular, *AbdB* being fully re-repressed (Fig. 3b; see below). Similar re-repression of the BX-C genes was observed in $Pc^{-/-}$ clones in imaginal discs, under restoration of normal PC levels[21]. We found that transcriptional re-repression of 'PC-rescued' cells is clearly stronger at PREs (Fig. 3c). The 3C analysis performed on these cells revealed that distal PRE–promoter interactions were restored as a function of the degree of re-repression (Fig. 3d). The *AbdB* promoter completely recovers its frequencies of interactions with all PREs (*Mcp*, *bxd* and *bx*), whereas *abdA* and *Ubx* promoters show an intermediate 'phenotype'.

A role for noncoding RNA in the formation of repressed heterochromatic domains has been postulated[22–26]. In *Drosophila*, components of the RNAi machinery are involved in PcG-mediated pairing-sensitive silencing (PSS) at the transgenic *Fab-7* element and in the production of small RNAs at this ectopic PRE[27]. In addition, the RNAi machinery influences the function and nuclear organization of the gypsy insulators[28]. To examine whether or not the interactions between epigenetic elements would be dependent on an RNA moiety, we treated S2 cells with RNase *in vivo* prior to 3C analysis, as previously described in mammalian cells[25]. We monitored RNase A digestion by following the glyceraldehyde-3 phosphate dehydrogenase (*gadph*) RNase by real-time PCR. As control after RNA extraction, the *gadph* transcript was reduced by 99% (data not shown), although the amount of DNA per cell remained unchanged after the treatment. The 3C analysis performed in parallel for cells treated or not with RNAse A led to the finding that PRE–PRE interactions and PRE–promoter interactions were not affected by the RNAse treatment (data not shown). We conclude that no structural RNA seems to be required for these interactions.

The relevance of higher-order structure formation and the functional state of other complex loci has been reported[29–31]. It has been shown that, following collinear activation of the murine HoxB cluster, active genes loop out of the repressed chromosome territory[32,33]. These findings strongly suggest that relocation of clustered genes occurs when *Hox* genes are actively transcribed. To investigate the higher-order structure of transcriptionally different tissues, we analysed the conformation of the BX-C locus in the *Drosophila melanogaster* cell line Schneider 3 (S3). S3 cells differ from S2 cells for the transcriptional state of the *AbdB* gene[19]. Analysis by real-time PCR revealed that, in the S3 cells used in this study, as in S2 cells, *Ubx* and *abdA* are repressed (or transcribed at low levels); in contrast to S2 cells, the three transcripts of *AbdB* are strongly transcribed (see Supplementary Information, Fig. S3d (ref 19). We have previously shown that, in all cases in S3 cells, no ABD-A or UBX proteins are made[19]. In S3 cells, *Fab-7* and *Mcp*, which control *AbdB* expression during development, are also strongly transcribed; *bxd* and *bx*, which control *Ubx*, show only basal transcription levels (see Supplementary Information, Fig. S3e).

Strikingly, 3C analysis revealed that, in S3 cells, *Fab-7* loses its physical interactions with most regions of the cluster (Fig. 4a); in particular, it loses its physical interactions with the *AbdB* γ and B/C promoters, whereas it maintains its interaction with the *AbdB* promoter A (which is the less active of the three promoters) (see Supplementary Information, Fig. S3d). This result confirms tethered DamID experiments in which *Fab-7* did not contact the active *AbdB* promoter[5]. To check if the *AbdB* transcription influences the 3D structure of repressed BX-C, we measured the cross-linking frequencies along the BX-C using the fixed fragment 42, which contains the *bxd* PRE element (Fig. 4b). In S3 cells, the *bxd* PRE element loses contact with the *AbdB* γ promoter, the *Fab-7* element and with the first part of the BX-C containing the *AbdB* gene, whereas the interactions with the rest of the locus remain unchanged. Similarly, when we used the fixed fragment in the *AbdB* γ promoter, we measured a drastic reduction in S3 cells of all the interactions found in S2 cells (see Supplementary Information, Fig. S5a). We tested the significance of the 3C profile differences between S2 and S3 conformation at BX-C by real-time PCR, measuring specific interactions (see Supplementary Information, Fig. S5b). The frequency of association between the *AbdB* γ promoter and *Fab-7* is reduced by more than 80% in S3 cells compared with S2 cells. Moreover, in S3 cells, the association of the *bxd* element with different BX-C fragments (*AbdB* γ promoter, *Fab-7* and *bx*) increases progressively from the active part of the BX-C towards the silent one. Thus, in S3 cells, the active *AbdB* γ promoter and the *Fab7* PRE are topologically separated from the rest of the other epigenetic elements of the locus.

To confirm these 3C results, we performed two-colour FISH analysis on S2 and S3 cultured cells (Fig. 4c). We used two combinations of FISH probes — *bxd*/*Fab-7* and *Fab-7*/*AbdB* promoter (*AbdBp*) — separated by approximately 66 kb. We found the two signals colocalized well in S2 cells. Interestingly, *Fab-7* interacts more frequently with *AbdBp* than with *bxd*. In S3 cells, the percentage of cells showing colocalization is significantly reduced, confirming the 3C analysis data and in agreement with the FISH analysis performed in embryos.

Our work provides evidence for three important facts: first, the silenced BX-C assumes a highly complex topology of the locus that involves all major PcG-regulated DNA elements, including PRE and promoter interactions and also long-distance PRE–PRE contacts (Fig. 5). Thus, PREs mediate higher-order structure formation.

Second, we found that natively active BX-C domains lose contact with the core of the repressed structure or PcG subnuclear domain. In particular, in cells that constitutively express the *AbdB* gene (S3 cells), the BX-C locus adopts different conformations in which active PREs and promoters lose the contact between each other and the repressive multi-looped core (Fig. 5). Thus, maintenance of the active state does not require direct interactions between PRE and the promoter. Moreover, we found that changes in the higher-order structure of the BX-C are accompanied by changes in nuclear position relative to PcG bodies (Fig. 1).

Third, we show that forced reactivation (Fig. 3) of the BX-C genes is not accompanied by strong antisilencing PRE transcription and that only the interactions between the active *AbdB*, *abdA* and *Ubx* promoters and their relative distal PREs are affected. Notably, this lack of change in proximal-PRE–promoter higher-order interactions seems to set the stage for subsequent re-repression as normal levels of PC are restored.

Finally, we have previously shown by ChIP analysis[19] that, in Pc-dsRNA-treated cells, as well as in S3 cells, transcriptional activation is accompanied by sensible changes in the epigenome structure — in particular, reduced levels of PC, PSC and PH, H3 Lys 9 di-/trimethylation and Lys 27 trimethylation, concomitant with an increase in Lys 4 di-/trimethylation and high levels of *Pol*II, TBP and elongation factors. Our work shows that these levels of epigenome changes are not sufficient to determine a stable epigenetic switch. Indeed it has been shown that major changes, on a genome-wide scale, of higher-order structures, in particular replicon and DNA loop organization, occur during differentiation and are required for reprogramming of cell identity[34]. We propose that the specific memory function exerted by PREs in the genome would be the result of their ability to integrate different levels of the epigenome, from histone modification to higher-order structures. □

## METHODS

**Culture cell growth.** S2 cells were grown in serum-free insect culture medium (HyQ SFX; Hyclone, Logan, UT). S3 cells were grown in Schneider's *Drosophila* medium (Gibco, Invitrogen, Carlsbad, CA) supplemented with 12.5% fetal bovine serum.

**Chromosome conformation capture (3C).** The 3C assay was performed essentially as described previously[35] with minor adaptations. The *Hind*III restriction enzyme, cutting 60 times in the 340 kb cluster, was used. The lengths of fragments obtained after digestion were between 500 bp and 3 kb. A total of $10^7$ cells were crosslinked in 45 ml of serum-free medium with 1% formaldehyde for 10 min at room temperature. The reaction was quenched by the addition of glycine to a final concentration of 0.125 M. Embryos were fixed as described previously[36]. Cells or embryos were centrifuged at 2000 rpm in an Eppendorf GS-6R centrifuge, resuspended in 1 ml of 4 °C cold cell lysis buffer (10 mM Tris pH 8.0, 10 mM NaCl, 0.2% NP40 and protease inhibitors), and incubated on ice for 15 min. Samples were kept on ice from this point onwards. Cell lysis was completed with ten strokes using a Dounce homogenizer (pestle A). Nuclei were washed with 0.5 ml of restriction enzyme buffer and pelleted. Nuclei were then resuspended in 362 µl of restriction enzyme buffer. SDS was added to a final concentration of 0.1%, and nuclei were incubated at 37 °C for 15 min. Triton X-100 was then added to the final concentration of 1% to sequester SDS. Digestion was performed with 400 U of restriction enzyme at 37 °C for 2 h. The restriction enzyme was inactivated by the addition of SDS to 2% and incubation at 65 °C for 30 min. The reaction was diluted into 8 ml ligation reaction buffer containing 1% Triton X-100, 50 mM Tris pH 7.5, 10 mM $MgCl_2$, 10 mM DTT, 0.1 mg $ml^{-1}$ bovine serum albumin, 1 mM ATP and 4000 U of T4 DNA Ligase (NEB, Ipswich, MA). Ligations were incubated at 16 °C for 2 h. EDTA (to a concentration of 10 mM) was added to stop the reactions. Samples were treated with 500 µg of Proteinase K and incubated for 5 h at 50 °C, and then overnight at 65 °C to reverse the formaldehyde crosslinks. The following day, the DNA was purified by phenol extraction and ethanol precipitation. Samples were redissolved in deionized water. To prepare a control template, we used four BACs spanning the entire 340 kb of the locus (3M20, 24L18, 48L13, 28H01). The DNA from each BAC was quantified by real-time PCR, using primers that anneal in the backbone. Equimolar amounts of the different BAC DNA were mixed and digested with the appropriate restriction enzyme, followed by ligation in 20 µl. The mix was purified by phenol extraction and ethanol precipitation. The sequences that were more represented (overlapping region of two contiguous BACs) were taken into consideration in the final calculation of crosslinking frequencies. Biological parameters, such as the heterogeneity of the cells, also have to be considered. Thus, when comparing two different cell types, we normalize to the total amount of DNA in the reaction, also considering the efficiency of digestion and ligation; this allows compensation of the varying efficiencies of the application due to the different source material. The efficiency of digestion after the entire 3C treatment was quantified by real-time PCR, amplifying a fragment spanning a *Hind*III site (uncut) in different 3C DNA preparations. To control the efficiency of ligation, a linear *Pst*I-digested plasmid was added to all the preparations before ligation. The ligated plasmid was quantified by real-time PCR, amplifying a fragment spanning the *Pst*I site. An appropriate amount of DNA that would amplify within the linear range was subsequently used for the experiments. A total of 30 rounds of PCR amplification were used. As standard, the 5' side of each restriction fragment was used to design primers. Primer sequences are available on request. PCR products were run on 2% agarose gels, stained with ethidium bromide and quantified with the Biorad Image Quant program (Biorad, Hercules, CA).

**Two-colour FISH and FISH-I on whole-mount tissues and cultured cells.** Two-colour FISH and FISH-I on embryos were performed as described previously[27] and a detailed protocol is available at http://www.epigenome-noe.net/research-tools/protocol.php?protid=5. For two-colour FISH on S2 or S3 cells, $10^6$ cells were centrifuged, resuspended in 0.4 ml of medium and placed for 30 min at room temperature on a poly-lysine-coated slide (22 mm × 22 mm). Fixation was performed in 4% paraformaldehyde and phosphate-buffered saline (PBS) for 10 min at room temperature. Cells were washed three times with PBT (PBS 1×, 0.1% Tween 20); incubated for 1 h at room temperature with RNAse A (100 µg $ml^{-1}$ in PBT); for 10 min at room temperature with PBS and 0.5% Triton; and for 30 min at room temperature in PBS and 20% glycerol. Cells were then frozen in liquid nitrogen and thawed at room temperature in PBS and 20% glycerol; this step was repeated four times. After washing the cells again in PBS, they were incubated for 5 min in 0.1 N HCl, briefly rinsed in 2×SSC, and stored in 50% formamide, 2×SSC, 10% dextransulphate, 50 mM sodium phosphate, pH 7.0. Fluorescent probes were prepared using the FISH Tag DNA Kit (Invitrogen, Carlsbad, CA), dissolved in the hybridization mixture (50% deionized formamide, 2×SSC, 10% dextransulphate, salmon sperm DNA at 0.5 mg $ml^{-1}$), applied to cells and sealed under coverslips with rubber cement. Probe and cellular DNA were denatured simultaneously on a hot block at 80 °C for 3 min. Hybridization was carried out in a humid atmosphere at 37 °C for 1 d. After hybridization, slides were washed in 2×SSC for 3 × 5 min at 37 °C, and in 0.1×SSC for 3 × 5 min at 45 °C, rinsed in PBS and counterstained with DAPI. The *AbdBp*, *bxd* and *Fab-7* FISH probes covered approximately 25 kb. Detailed coordinates of the genomic fragments used to produce these two probes are available on request from C.L. or F.B.

**RNase treatment.** Cells were centrifuged at 2000 rpm in an Eppendorf GS-6R centrifuge, washed in 5 ml of PBS 1×, resuspended in 5 ml of CSK buffer (100 mM NaCl, 300 mM sucrose, 3 mM $MgCl_2$, 10 mM PIPES, pH 7.3) supplemented with 0.5% Triton X-100, 1× protease inhibitors, 1 mM PMSF and incubated at room temperature for 15 min. The Triton-X-100-permeabilized cells were washed in 5 ml of PBS 1×, resuspended in 5 ml of PBS 1× with or without 0.1 mg $ml^{-1}$ RNase A (Roche, Basel, Switzerland) and incubated at room temperature for 10 min. Cells were centrifuged and resuspended in 45 ml of culture medium (HyQ SFX; Hyclone) and processed for 3C analysis.

**Statistical analysis.** To compare the means of multiple crosslinking frequencies and to detect significant differences between them, we applied analysis of variance (ANOVA). A one-way ANOVA was applied to a single-cell population to test the differences between groups that are classified based on one independent variable (the crosslinking frequencies). Alternatively, to compare different cell lines, we used two-way ANOVA without replication on the crosslinking frequencies averages.

**Real-time PCR analysis.** Total RNA was isolated with Trizol reagent (Invitrogen). An aliquot of 1 μg of RNA from each sample was subjected to cDNA synthesis using a Quantiteck reverse transcription kit (Qiagen, Hilden, Germany). A total of 2 μl of cDNA preparation was amplified in 20 μl reaction mixtures in the presence of 10 μl 2× QuantiTect SYBR Green master mix (Qiagen) and 0.5 μM of corresponding primers. Primers were designed to eliminate the detection of genomic DNA. Primer sequences are available on request. All primers were annealed at 60 °C. Real-time PCR was performed with the DNA Engine Opticon 2 (MJ) controlled by Opticon Monitor 2 software (MJ). Copy number was determined using the cross-point (Cp) value, which is automatically calculated using the Opticon Monitor 2 software (MJ). The relative Cp value was determined for each transcript using the cross-point (Cp) value of the housekeeper gene (*GADPH*) performed with the same batch of master mix.

**RNAi.** Exonic fragments of 1400 bp or 600 bp, respectively, from *Pc* or *Gfp* genes were amplified by PCR, creating T7 polymerase binding sites for the transcription of both strands. RNAi was performed as described previously[20]. (Pc primers — F: ACATCCTGGATCGCCGCCTCA; R: ATTGGCAAGTTAAGCACGGGCA. Gfp primers — F: ACGTAAACGGCCACAAGTTC; R:TGCTCAGGTAGTGGTTGTCG).

*Note: Supplementary Information is available on the Nature Cell Biology website.*

ACKNOWLEDGEMENTS

We thank G. Cavalli for providing lab space and funding to perform the work done by F.B. and V.R., stimulating discussions and constructive criticisms about this manuscript. We thank A. Breiling, G. Oliva, N. Hornig, M. Vivo, Z. Jasencakova, M. Matarazzo and F. Cernilogar for helpful comments on the manuscript and technical advice. We are grateful to A. Ambesi-Impiombato, D. Di Bernardo, A. Buonocore, E. Pirozzi and A. Mas for statistical analysis, and to D. Romano for modelling the 3D image. This work was supported by grants from Fondazione Telethon (TCP00094), La Compagnia di San Paolo, Associazione Italiana Ricerca sul Cancro AIRC, VolkwagenStiftung (I77 996) and The Epigenome Network of Excellence (LSHG-CT-2004-503433) to V.O.; by the National Institutes of Health (HG03143) to J.D. V.R. is supported by the Ministère de la Recherche, F.B. is supported by the CNRS. C.L. and V.O. would like to dedicate this work to the heart and soul of Maria Graziella Persico.

AUTHOR CONTRIBUTIONS

C.L. performed all 3C experiments, FISH analysis on *Drosophila* S2 and S3 cells and part of statistical analysis. V.R. and F.B. performed FISH experiments on embryos and helped C.L. with FISH analysis in S2 and S3 cells. J.D. provided unpublished protocols on 3C technology and suggested crucial control experiments. V.O. designed the experiments, participated in data analysis and presentation, and prepared the manuscript together with C.L. At all stages, all authors discussed the results and gave a substantial contribution to the final manuscript.

Published online at http://www.nature.com/naturecellbiology/
Reprints and permissions information is available online at http://npg.nature.com/reprintsandpermissions/

1. Schuettengruber, B., Chourrout, D., Vervoort, M., Leblanc, B. & Cavalli, G. Genome regulation by polycomb and trithorax proteins. *Cell* **128,** 735–745 (2007).
2. Orlando, V. Polycomb, epigenomes and control of cell identity. *Cell* **112,** 591–606 (2003).
3. Levine, S. S., King, I. F. & Kingston, R. E. Division of labor in polycomb group repression. *Trends Biochem. Sci.* **29,** 478–485 (2004).
4. Bantignies, F., Grimaud, C., Lavrov, S., Gabut, M. & Cavalli, G. Inheritance of Polycomb-dependent chromosomal interactions in *Drosophila*. *Genes Dev.* **17,** 2406–2420 (2003).
5. Cleard, F., Moshkin, Y., Karch, F. & Maeda, R. K. Probing long-distance regulatory interactions in the *Drosophila melanogaster* bithorax complex using Dam identification. *Nature Genet.* **38,** 931–935 (2006).
6. Comet, I. *et al*. PRE-mediated bypass of two Su(Hw) insulators targets PcG proteins to a downstream promoter. *Dev. Cell* **11,** 117–124 (2006).
7. Pirrotta, V. PcG complexes and chromatin silencing. *Curr. Opin. Genet. Dev.* **7,** 249–258 (1997).
8. Lanzuolo, C. & Orlando, V. The function of the epigenome in cell reprogramming. *Cell. Mol. Life Sci.* **64,** 1043–1062 (2007).
9. Petruk, S. *et al*. Transcription of bxd noncoding RNAs promoted by trithorax represses Ubx in *cis* by transcriptional interference. *Cell* **127,** 1209–1221 (2006).
10. Rank, G., Prestel, M. & Paro, R. Transcription through intergenic chromosomal memory elements of the *Drosophila* bithorax complex correlates with an epigenetic switch. *Mol. Cell. Biol.* **22,** 8026–8034 (2002).
11. Schmitt, S., Prestel, M. & Paro, R. Intergenic transcription through a polycomb group response element counteracts silencing. *Genes Dev.* **19,** 697–708 (2005).
12. Ronshaugen, M. & Levine, M. Visualization of trans-homolog enhancer-promoter interactions at the Abd-B Hox locus in the *Drosophila* embryo. *Dev. Cell* **7,** 925–932 (2004).
13. Vazquez, J., Muller, M., Pirrotta, V. & Sedat, J. W. The Mcp element mediates stable long-range chromosome-chromosome interactions in *Drosophila*. *Mol. Biol. Cell* **17,** 2158–2165 (2006).
14. Gasser, S. M. Visualizing chromatin dynamics in interphase nuclei. *Science* **296,** 1412–1416 (2002).
15. Lanctot, C., Cheutin, T., Cremer, M., Cavalli, G. & Cremer, T. Dynamic genome architecture in the nuclear space: regulation of gene expression in three dimensions. *Nature Rev. Genet.* **8,** 104–115 (2007).
16. Misteli, T. Beyond the sequence: cellular organization of genome function. *Cell* **128,** 787–800 (2007).
17. Buchenau, P., Hodgson, J., Strutt, H. & Arndt-Jovin, D. J. The distribution of polycomb-group proteins during cell division and development in *Drosophila* embryos: impact on models for silencing. *J. Cell Biol.* **141,** 469–481 (1998).
18. Ficz, G., Heintzmann, R. & Arndt-Jovin, D. J. Polycomb group protein complexes exchange rapidly in living *Drosophila*. *Development* **132,** 3963–3976 (2005).
19. Breiling, A., O'Neill, L. P., D'Eliseo, D., Turner, B. M. & Orlando, V. Epigenome changes in active and inactive polycomb-group-controlled regions. *EMBO Rep.* **5,** 976–982 (2004).
20. Breiling, A., Turner, B. M., Bianchi, M. E. & Orlando, V. General transcription factors bind promoters repressed by Polycomb group proteins. *Nature* **412,** 651–655 (2001).
21. Beuchle, D., Struhl, G. & Muller, J. Polycomb group proteins and heritable silencing of *Drosophila* Hox genes. *Development* **128,** 993–1004 (2001).
22. Fukagawa, T. *et al*. Dicer is essential for formation of the heterochromatin structure in vertebrate cells. *Nature Cell Biol.* **6,** 784–791 (2004).
23. Kanellopoulou, C. *et al*. Dicer-deficient mouse embryonic stem cells are defective in differentiation and centromeric silencing. *Genes Dev.* **19,** 489–501 (2005).
24. Lippman, Z. & Martienssen, R. The role of RNA interference in heterochromatic silencing. *Nature* **431,** 364–370 (2004).
25. Maison, C. *et al*. Higher-order structure in pericentric heterochromatin involves a distinct pattern of histone modification and an RNA component. *Nature Genet.* **30,** 329–334 (2002).
26. Volpe, T. A. *et al*. Regulation of heterochromatic silencing and histone H3 lysine-9 methylation by RNAi. *Science* **297,** 1833–1837 (2002).
27. Grimaud, C. *et al*. RNAi components are required for nuclear clustering of Polycomb group response elements. *Cell* **124,** 957–971 (2006).
28. Lei, E. P. & Corces, V. G. RNA interference machinery influences the nuclear organization of a chromatin insulator. *Nature Genet.* **38,** 936–941 (2006).
29. de Laat, W. & Grosveld, F. Spatial organization of gene expression: the active chromatin hub. *Chromosome Res.* **11,** 447–459 (2003).
30. Kumar, P. P. *et al*. Functional interaction between PML and SATB1 regulates chromatin-loop architecture and transcription of the MHC class I locus. *Nature Cell Biol.* **9,** 45–56 (2007).
31. Kurukuti, S. *et al*. CTCF binding at the H19 imprinting control region mediates maternally inherited higher-order chromatin conformation to restrict enhancer access to Igf2. *Proc. Natl Acad. Sci. USA* **103,** 10684–10689 (2006).
32. Chambeyron, S. & Bickmore, W. A. Chromatin decondensation and nuclear reorganization of the HoxB locus upon induction of transcription. *Genes Dev.* **18,** 1119–1130 (2004).
33. Chambeyron, S., Da Silva, N. R., Lawson, K. A. & Bickmore, W. A. Nuclear re-organisation of the Hoxb complex during mouse embryonic development. *Development* **132,** 2215–2223 (2005).
34. Lemaitre *et al*., Mitotic remodeling of the replicon and chromosome structure. *Cell* **123,** 787-801 (2005)
35. Dekker, J., Rippe, K., Dekker, M. & Kleckner, N. Capturing chromosome conformation. *Science* **295,** 1306–1311 (2002).
36. Orlando, V., Jane, E. P., Chinwalla, V., Harte, P. J. & Paro, R. Binding of trithorax and Polycomb proteins to the bithorax complex: dynamic changes during early *Drosophila* embryogenesis. *EMBO J.* **17,** 5141–5150 (1998).